Journal of the Meteorological Society of Japan, Vol. 94A, pp. 199−208, 2016
DOI:10.2151/jmsj.2015-046

NOTES AND CORRESPONDENCE

Historical Dynamical Downscaling for East Asia with the Atmosphere and Ocean Coupled Regional Model

Suryun HAM

Atmosphere and Ocean Research Institute, The University of Tokyo, Kashiwa, Japan

Kei YOSHIMURA

Atmosphere and Ocean Research Institute, The University of Tokyo, Kashiwa, Japan
Institute of Industrial Science, The University of Tokyo, Chiba, Japan

and

Haiqin LI

NOAA Earth System Research Laboratory, Colorado, USA
Cooperative Institute for Research in Environmental Sciences, University of Colorado, Colorado, USA

(Manuscript received 11 December 2014, in final form 30 July 2015)

Abstract

The atmosphere–ocean-coupled regional downscaling system of the Regional Spectral Model for the atmosphere and the Regional Ocean Modeling System (RSM–ROMS) was used to improve the downscaling simulation accuracy, particularly of coastal areas, and a dynamical downscale of the historical global reanalysis data for the East Asian region over 25 years was conducted. The results showed that in the coupled run, the sea surface temperature (SST) tended to show large-scale discrepancy from reality, basically because the models remain imperfect. On the other hand, for net heat flux, precipitation, and surface air temperature, the coupled run showed positive improvement compared with the uncoupled run. The improvement in these three variables and the degradation in SST were also apparent for event-based (one-month) averages. This inconsistency between the impacts on SST and the other variables may indicate that there is room to improve the model system further, particularly in the coupling and/or boundary layer processes for both the atmosphere and ocean.

Keywords RSM–ROMS; atmosphere–ocean coupling; high-resolution SST

1. Introduction

Since the pioneering work of Giorgi and Bates (1989), the dynamical downscaling technique with high-resolution regional atmospheric models has been used for various purposes, including seasonal weather forecasts (e.g., Yoon et al. 2012), identification of

Corresponding author: Kei Yoshimura, Atmosphere and Ocean Research Institute, The University of Tokyo, 5-1-5 Kashiwanoha, Kashiwa, Chiba 277-8568, Japan
E-mail: kei@aori.u-tokyo.ac.jp

Table 1. Previous development of regional atmosphere–ocean-coupled model systems.

Reference	System Name	Atmospheric model	Oceanic model	Target Region
Hodur 1997	COAMPS	COAMPS Atmos model	COAMPS ocean model	Pacific side of North America
Gustafsson et al. 1998		HIRLAM	BOBA-PROBE	Baltic Sea
Powers and Stoelinga 2000		MM5	POM	Lake Erie
Döscher et al. 2002	RCAO	RCA (HIRLAM)	RCO (OCCAM)	Europe
Schrum et al. 2003		REMO	HAMSOM	Baltic Sea
Sasaki et al. 2006	MRI-CRCM	MRI-RSM	NPOGCM	Japan
Seo et al. 2007	SCOAR	RSM	ROMS	Western Pacific
Xie et al. 2007	iROAM	iRAM	MOM2	Western Pacific
Zou and Zhou 2011	FROALS	RegCM3/CREM	POM2000	Northwestern Pacific
Li et al. 2012		RSM	ROMS	Pacific side of North America
Samala et al. 2013		WRF	ROMS	Indian Ocean

land–atmosphere interactions (e.g., DeHaan and Kanamitsu 2008), the orographic process of rainfall patterns (e.g., Leung and Ghan 1995), and behavior of typhoons (e.g., Minamide and Yoshimura 2014). In addition to these various purposes, dynamical downscaling is regarded as one of the most promising tools for regional climate projection. However, the problem of using low-resolution lower boundary conditions, particularly sea surface temperature (SST), has been pointed out (Li et al. 2012). The use of the atmosphere–ocean (hereafter abbreviated as A–O)-coupled regional model is one of the solutions (Hong and Kanamitsu 2014).

The studies of the A–O-coupled regional model are not new but not too old. The initial work was done by Hodur (1997), who developed the Coupled Ocean/Atmosphere Mesoscale Prediction System (COAMPS) targeting the Pacific side of the North American continent. Since then, as listed in Table 1, approximately 10 systems have been developed. Some of the model systems are not currently in use, but a few of them are available. As one of the more recently developed model systems, the Regional Spectral Model–Regional Ocean Model System (RSM–ROMS), which was developed by Li et al. (2012), was used for A–O-coupled dynamical downscaling simulations over the western part of North America for the historical period using reanalysis data (Li et al. 2012) and for present and future climate using the National Center for Atmospheric Research (NCAR) Community Climate System Model version 3 (CCSM3) output (Li et al. 2014a, b). These studies revealed that the impact of using high-resolution and physically interactive lower boundary conditions was indeed significant for future climate prediction over coastal regions, particularly the Bay Area of California. This regional coupled model was also applied for reanalysis-coupled downscaling over the Intra-Americas Seas (Li and Misra 2014). A highlight of coupled downscaling is its resolving of the loop current and its associated eddy shedding and variance of sea surface height, which is poorly simulated in the Climate Forecast System Reanalysis (CFSR; Saha et al. 2010). However, RSM–ROMS has not yet been tested for other regions. Therefore, this note briefly presents an application of RSM–ROMS for A–O-coupled dynamical downscaling simulations for the East Asia region during the historical period.

2. Description of the model and experiments

2.1 RSM–ROMS

Li et al. (2012) coupled the Scripps Institution of Oceanography version of RSM (Kanamitsu et al. 2005) and the ROMS version 3 (Shchepetkin and McWilliams 2005), naming the coupled system RSM–ROMS. The model components are the same as those of the Scripps Coupled Ocean–Atmosphere Regional (SCOAR) model (Seo et al. 2007), but there are significant practical improvements such as in the user interface, domain specification friendliness, and parallel computing optimization.

The hydrostatic regional atmospheric model RSM has been used in many studies (e.g., Ham et al. 2015). In the present study, we used the following for the major physical processes: the simplified Arakawa-Schubert scheme (Hong and Pan 1998) for convective parameterization, a diagnostic microphysics scheme (Hong et al. 1998), the Noah land surface model (Ek et al. 2003), shortwave (Chou 1992) and longwave (Chou et al. 1999) radiation

parameterizations, and a non-local boundary layer scheme (Hong and Pan 1996). Additionally, we adopted the new spectral nudging scheme developed by Hong and Chang (2012) to apply the lateral boundary conditions. Thanks to extensive efforts by previous developers, RSM has come to be regarded as a major regional climate model through many multi-model intercomparison studies (e.g., Pierce et al. 2013).

ROMS is a free-surface, terrain-following, primitive equation ocean model. A large number of studies have used ROMS, including the one using it coupled with the Weather Research and Forecasting (WRF) model by Samala et al. (2013). We used version 3.0 with the level 2.5 Mellor–Yamada mixing scheme (Mellor and Yamada 1982), the K-profile boundary layer scheme (Large et al. 1994), and built-in flux correction (Marchesiello et al. 2003).

2.2 *Experiment setup*

The target region mainly includes Japan, Korea, the eastern part of China, and surrounding oceans, as shown in Fig. 1, and 20-km horizontal resolution in Mercator projection (115.124°E–154.999°E and 25.592°N–55.955°N; 192 × 199 grids), 28 sigma-level layers in the atmosphere, and 30 sigma-level layers in the ocean were used. The integration period was from 1980 to 2005, and the results from the last 20 years (1986–2005) were used for analyses. The atmospheric lateral boundary conditions were derived from the National Center for Environmental Prediction (NCEP)/US Department of Energy (DOE) Reanalysis 2 (hereafter RA2; Kanamitsu et al. 2002). As a surface boundary condition for the A–O-uncoupled run, the Optimum Interpolated SST (OISST) data with a resolution of 1 degree (Reynolds and Smith 1994) were used. The ocean lateral boundary condition for the A–O-coupled run was obtained from the monthly Simplified Ocean Data Assimilation (SODA; Carton et al. 2000). The information exchange between the atmosphere and ocean for the A–O-coupled experiment takes place every 24 h. Due to differences in computation loads, 20 CPUs were assigned for the atmospheric simulation and 4 CPUs were assigned for the ocean. Hereafter, the A–O-coupled experiment is referred to as CPL, and the same run but without ROMS is referred to as UNCPL.

2.3 *Data used for validation*

For validation, we used the daily OISST version 2 with Advanced Very High Resolution Radiometer (AVHRR) only in resolution of 0.25 degrees (Reynolds et al. 2007), surface net heat fluxes radiation data from the Objectively Analyzed air–sea Fluxes (OAFlux; http://oaflux.whoi.edu), and precipitation and surface air temperature data from the Asian Precipitation - Highly - Resolved Observational Data Integration Towards Evaluation of the Water Resources (APHRODITE) data sets (http://www.chikyu.ac.jp) (Yatagai et al. 2012).

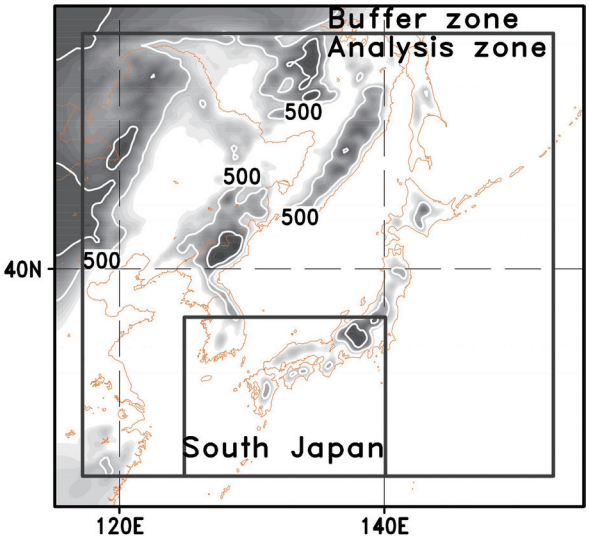

Fig. 1. Domain specification of this study. Both shades and contours indicate orography(m). The innermost rectangle was used for short-term event-based comparison.

3. Results

3.1 *Validation at climatological scale*

Figure 2 shows the 20-year climatological June–July–August (JJA) averages for SST, surface net heat fluxes over oceans, and precipitation distribution compared with corresponding observations. For SST, because the UNCPL experiments used observation data with low resolution (1° × 1°) (Fig. 2b), these distributions are more similar to those of the AVHRR analyses with high resolution (0.25° × 0.25°) (Fig. 2a) than those of the CPL experiments (Fig. 2c). The pattern correlation (PC) coefficients are almost the same (0.99 for both UNCPL and CPL), but the root mean square error (RMSE) is degraded from 0.39°C in UNCPL to 1.29°C in CPL. The overall degradation in SST is somewhat inevitable due to the fact that both RSM and ROMS are imperfect. However, as shown in Fig. 2d, CPL SST shows some temperature decrease along the coastlines compared with UNCPL, particularly along east China (Tsingtao to Shanghai),

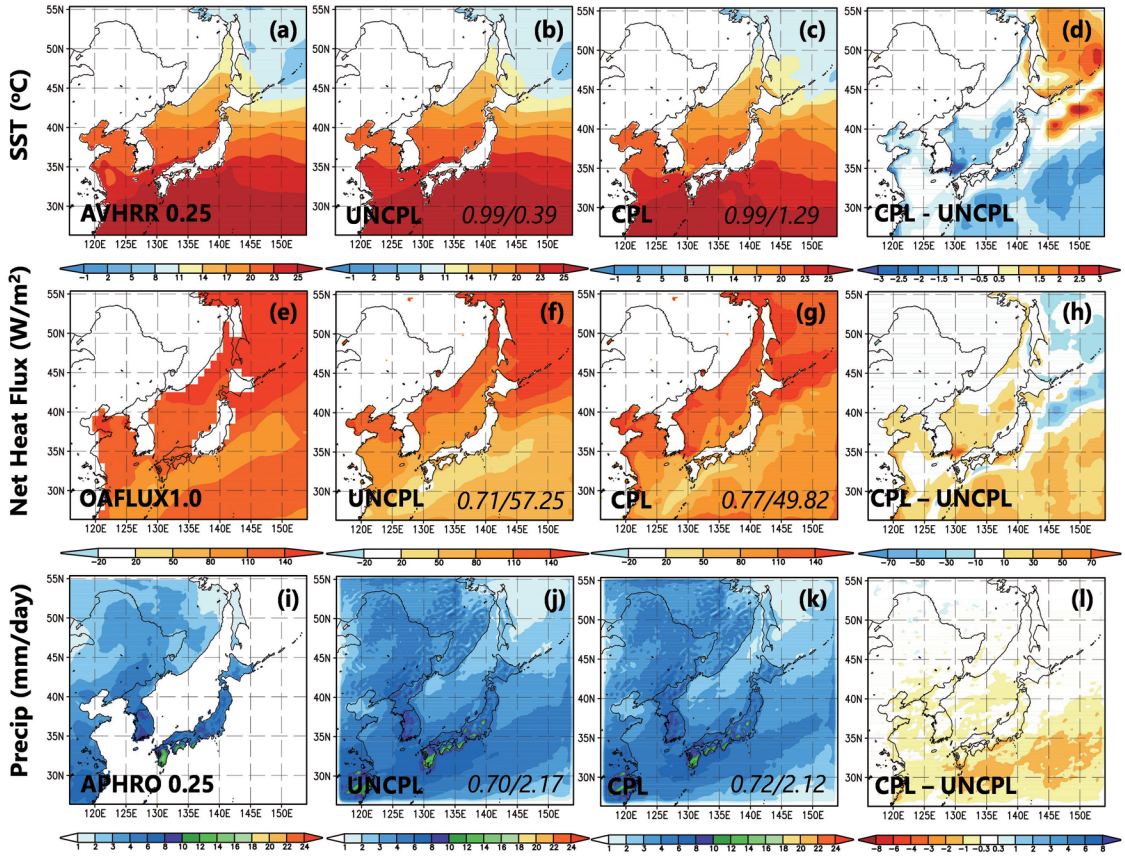

Fig. 2. Climatological June–July–August (JJA) means of sea surface temperature (SST) (top row; a–d), net heat flux (middle row; e–h), and precipitation (bottom row; i–l). The observation data are shown in the leftmost column (a, e, and i); the uncoupled experiment (UNCPL) results are shown in the second left column (b, f, and j), the coupled experiment (CPL) results are shown in the second right column (c, g, and k), and differences between UNCPL and CPL (CPL minus UNCPL) are shown in the rightmost column (d, h, and l). The numbers in the left three columns indicate the pattern correlation (PC) and root mean square error (RMSE) of each run against the observations. The simulated net heat flux (positive downward) is calculated by the radiation fluxes and latent/sensible heat fluxes at the surface.

east Russia (Nevelskoy Strait), and the Pacific side of Japan. These SST decreases are due to Ekman uplifting currents near the coast caused by near-surface wind and current. SST cooling is also related to some biases from the atmospheric model, such as in precipitation, cloudiness, and surface net heat fluxes (Ham et al. 2014; Zou and Zhou 2011). Ham et al. (2014) found that SST cooling is linked to positive precipitation biases by increased cloudiness and the blocking of solar radiation. Zou and Zhou (2011) suggested SST cold bias due to overestimation of the convection frequency of the atmospheric model. Also, SST from CPL run might be cooled to keep the balance of the fluxes.

Contrary to SST, surface net heat flux (positive downward) in CPL (Fig. 2g) shows better overall agreement with the observation (Fig. 2e) than that in UNCPL (Fig. 2f) for both PC (0.71 to 0.77) and RMSE (57 W m^{-2} to 50 W m^{-2}). There is systematic underestimation over most of the oceans in UNCPL, but the underestimation is improved to some extent in CPL, except at the northeastern part of the target domain (Fig. 2h). A distinct difference between CPL and UNCPL can be found along the Kuroshio Current, one of the largest ocean streams in the world. This fact indicates the representation of physically reasonable interaction between the atmosphere and ocean in the A–O-coupled model. Thus, it is worth mentioning

Table 2. June to August of 1986 averaged sea surface latent heat flux (positive downward), sensible heat flux (positive downward), shortwave radiation flux (positive downward), longwave radiation flux (positive downward), and net heat flux (positive downward) averaged over the analysis zone.

	OAFlux/ISCCP	UNCPL	CPL
Latent heat (W m^{-2})	–28.2	–62.6	–51.5
Sensible heat (W m^{-2})	–3.4	–12.0	–12.2
Shortwave radiation (W m^{-2})	194.2	177.2	176.1
Longwave radiation (W m^{-2})	–41.8	–35.7	–35.6
Net heat (W m^{-2})	120.8	66.9	76.8

that a better representation of heat flux is not always associated with a better representation of SST. This implies room for further improvement in the coupling processes and the representation of boundary layers in either the atmosphere or ocean model or both.

For precipitation, the impact is not too large, but there does seem to be a positive impact. Compared with the observation over land (Fig. 2i), PC slightly increases from 0.70 to 0.72, and RMSE decreases from 2.2 mm day^{-1} to 2.1 mm day^{-1} (Figs. 2j, k). A comparison with the Global Precipitation Climatology Project (GPCP) dataset (Huffman et al. 2001), which covers both land and ocean, also showed a similar tendency (figure not shown). The largest difference between CPL and UNCPL, which is associated with a decrease in SST and an increase in net heat flux, is over the Pacific Ocean. The impact is quite large, so there are some impacts in the coastal regions, particularly the Pacific side of Japan and the east coastal part of China.

Interestingly, the surface net heat flux difference tends to be closely related to SST and precipitation difference patterns (Figs. 2d, h, l). Table 2 shows the summer of 1986 averaged sea surface fluxes budget averaged over the domain. Although this represents the averaged values of only one year, it is enough to understand the difference between CPL and UNCPL compared with the observation. The wet pattern can be linked to the negative heat flux difference caused by increased cloudiness and blocking of solar radiation (shortwave fluxes from UNCPL are underestimated compared with the observation; Table 2). The negative heat flux biases cool the ocean surface and induce additional SST cooling. However, the atmosphere-only model (for the UNCPL simulation) cannot reflect this process because it uses the observed forced SST, which does not consider the ocean–atmosphere interaction. These findings confirm that in the results from the UNCPL simulation, the net surface heat fluxes from the UNCPL simulation show underestimation compared with the observed OAFLUX data. In contrast to the atmosphere-only model, the coupled model (for the CPL simulation) includes the ocean–atmosphere feedback process. Therefore, SST cooling in the coupled model leads to an increase in net heat fluxes and a decrease in precipitation compared with the results of the uncoupled model (Figs. 2d, h, l), which is related to the reduced latent heat fluxes (Table 2). Here, reduced latent heat fluxes in the CPL experiment are mainly due to the humidity change. Meanwhile, the change in wind speed by the coupled system is not significant (figure not shown). Although simulated net heat fluxes in the CPL experiment are increased compared with those in the UNCPL experiment, they are still underestimated in comparison with those in the observation. This would induce the cold SST biases. These findings are consistent with those of Ham et al. (2014), although they used the global coupled model. They suggested that the coupling system led to improvement in the surface net heat flux and precipitation due to reasonable air–sea interaction despite the cold biases of SST. Additionally, Zou and Zhou (2012) indicated that simulation with regional air–sea coupling improved the simulation of net heat flux over the ocean, particularly for latent heat flux, despite the SST biases.

Figure 3 is the same as Fig. 2, except that it shows the climatological December–January–February (DJF) season. Similar to the summer case, there is a larger bias in SST, although there are small-scale features in CPL. The overestimation of SST occurs over the north coastal part of Japan, the Yellow Sea, and south of the Chishima Islands in CPL. PC decreases from 0.98 to 0.96, and RMSE increases from 2.4°C to 2.7°C. Despite the SST discrepancies, net heat flux is significantly improved. PC increases from 0.70 to 0.82 in CPL, and RMSE decreases to 60 W m^{-2} from 72 W m^{-2}. This difference is due to

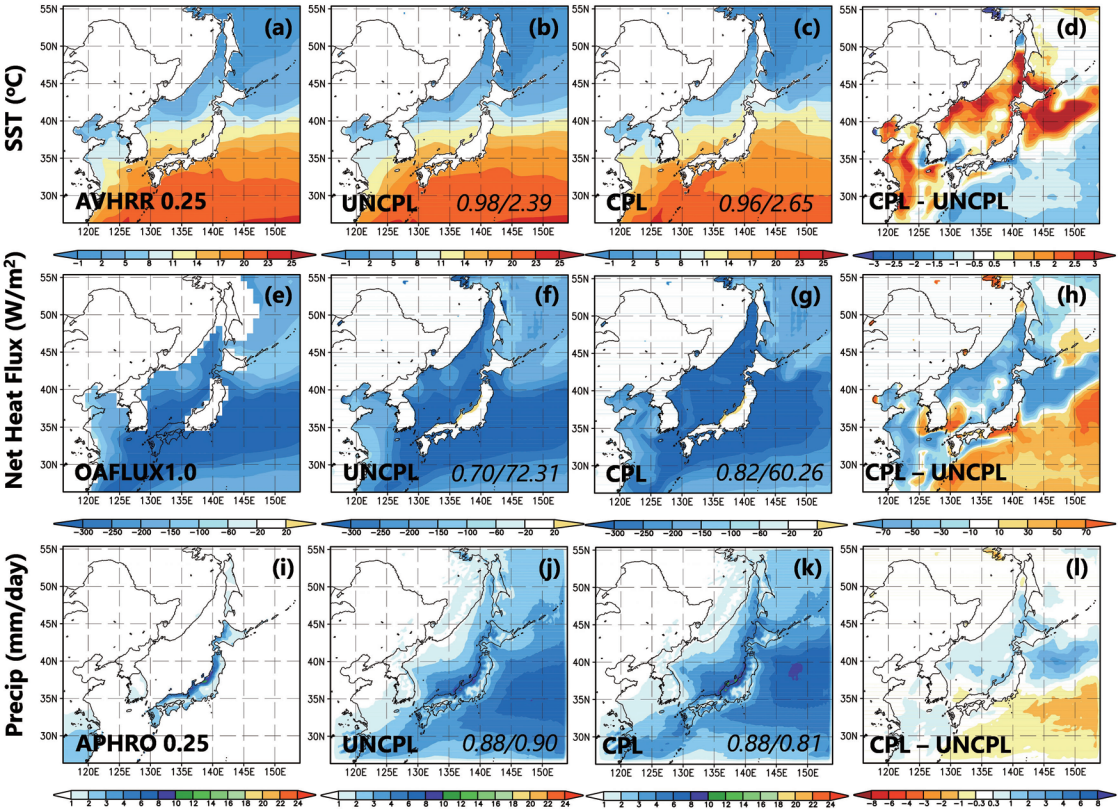

Fig. 3. Same as Fig. 2, but for December–January–February (DJF) climatology.

the fact that the little cooling (less negative values) in UNCPL in the Yellow Sea, East China Sea, and north coastal part of Japan is improved by CPL with physically reasonable interaction between the atmosphere and ocean. The difference between CPL and UNCPL over the Pacific is divided by the Kuroshio Current and its extension currents. Over the area south of the Kuroshio, net heat flux is less negative (less ocean cooling) in CPL. For precipitation, as was the case for summer, the impact is somewhat limited, but in a good direction. RMSE decreases from 0.90 to 0.81 mm day^{-1}, whereas the correlation remains the same. The impacted area is associated with SST and heat flux changes, particularly over the Pacific.

Figure 4 shows the seasonal changes in area mean SST (Fig. 4a), surface air temperature (SAT) (Fig. 4b), surface net heat flux (Fig. 4c), and precipitation (Fig. 4d). Note that SST and net heat flux are over the ocean, whereas SAT and precipitation are over the land only. Contrary to the degradation in spatial correlation and RMSE in SST shown in the previous figures, the regional average SST showed some improvement, particularly in the summer months. The impact of coupling is not always in a better direction for averaged SST, particularly in the winter season. Surprisingly, the coupling almost always improves results for all other variables. For example, for SAT, the warm biases (maximum of about 1.5°C) in the summer months were slightly decreased (maximum of about 1.3°C), whereas no significant change occurred in the winter months, although there are obvious cool biases with a maximum of more than 2°C in both experiments. For net heat flux, the problems of too little heating (less positive) in summer months and too little cooling (less negative) in winter months are both improved. The case is similar for precipitation, for which too much (too little) precipitation in winter (summer) months is slightly improved.

3.2 *Validation at event-based scale*

To examine the impact of a single event (or a few events) more carefully, we arbitrarily select July 1987 when Typhoon Thelma struck the south of Korea and the Kyushu area of Japan. Similar to Figs. 2 and 3,

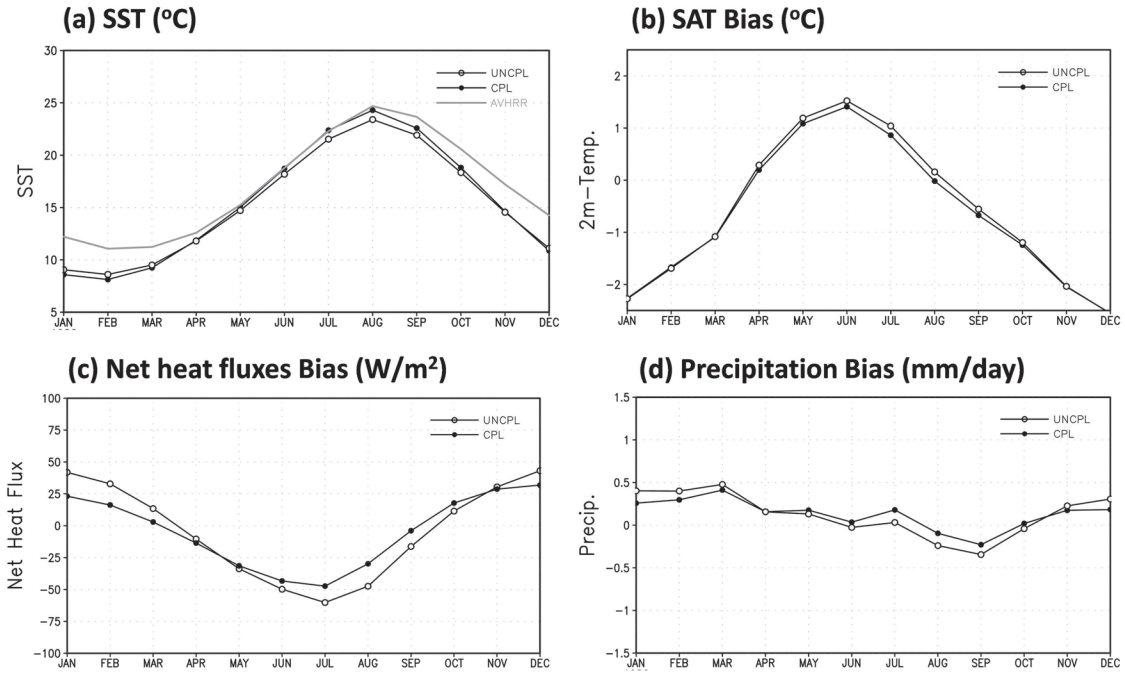

Fig. 4. Seasonality of area mean climatological variables: (a) SST, (b) surface air temperature (SAT), (c) net heat flux, and (d) precipitation. The absolute values of model runs and Advanced Very High Resolution Radiometer (AVHRR) observation (gray line) are shown for only for SST. Open symbols are UNCPL, and closed symbols are CPL.

Fig. 5 shows SST, net heat flux, SAT, and precipitation, but over the more focused region of Korea and southern Japan (designated in Fig. 1). The SST field changes to a finer structure in the CPL run (Fig. 5c). Again, similar to climatological analyses, the difference in SST does not necessarily produce better agreement with the high-resolution AVHRR observation (Fig. 5a) compared with the low-resolution UNCPL forcing (Fig. 5b). PC decreases from 0.97 to 0.89, and RMSE increases from 0.56°C to 1.18°C. However, the AVHRR data obviously show spatially finer structure associated with the Kuroshio Current, as shown in CPL. An apparent difference between UNCPL and CPL can be seen as cooling in the Tsushima Strait, where much precipitation occurred as a result of the typhoon.

On the other hand, the performance for net heat flux, SAT, and precipitation is almost always improved or unchanged. There is too little heating over almost the entire domain by the UNCPL run, but the CPL run improves this negative bias over the entire domain, although both PC and RMSE are not very good (0.27 to 0.35 and 47.9 W m^{-2} to 44.9 W m^{-2}, respectively). For SAT, the impact is very limited (both PC and RMSE do not change much: 0.81 to 0.84 for PC and 1.22 to 1.23 mm day^{-1} for RMSE). The biggest difference is over the ocean, such as SST (Fig. 5d), but it also shows a little impact over the land. For precipitation over the land, there is some impact by CPL, with both PC and RMSE being slightly improved (0.57 to 0.58 for PC, 16.2 mm day^{-1} to 16.1 mm day^{-1} for RMSE). There is a small precipitation decrease in the Tsushima Strait and in corresponding coastal areas of Korea and Japan, which is mainly due to SST cooling by CPL, indicating the possibility of overestimation by the UNCPL run, because the cooling effect by heavy precipitation was not taken into account.

The impact of air–sea interaction for single event may be sensitive to each event. For example, Wada and Usui (2007) investigated the impact of oceanic processes on typhoons and pointed out that it was sensitive to individual cases. In this study, some typhoon cases related to the target region were additionally investigated (not shown). It is clear that the CPL experiment produces almost the same improvement for atmospheric variables such as surface net heat fluxes and precipitation by SST cooling in

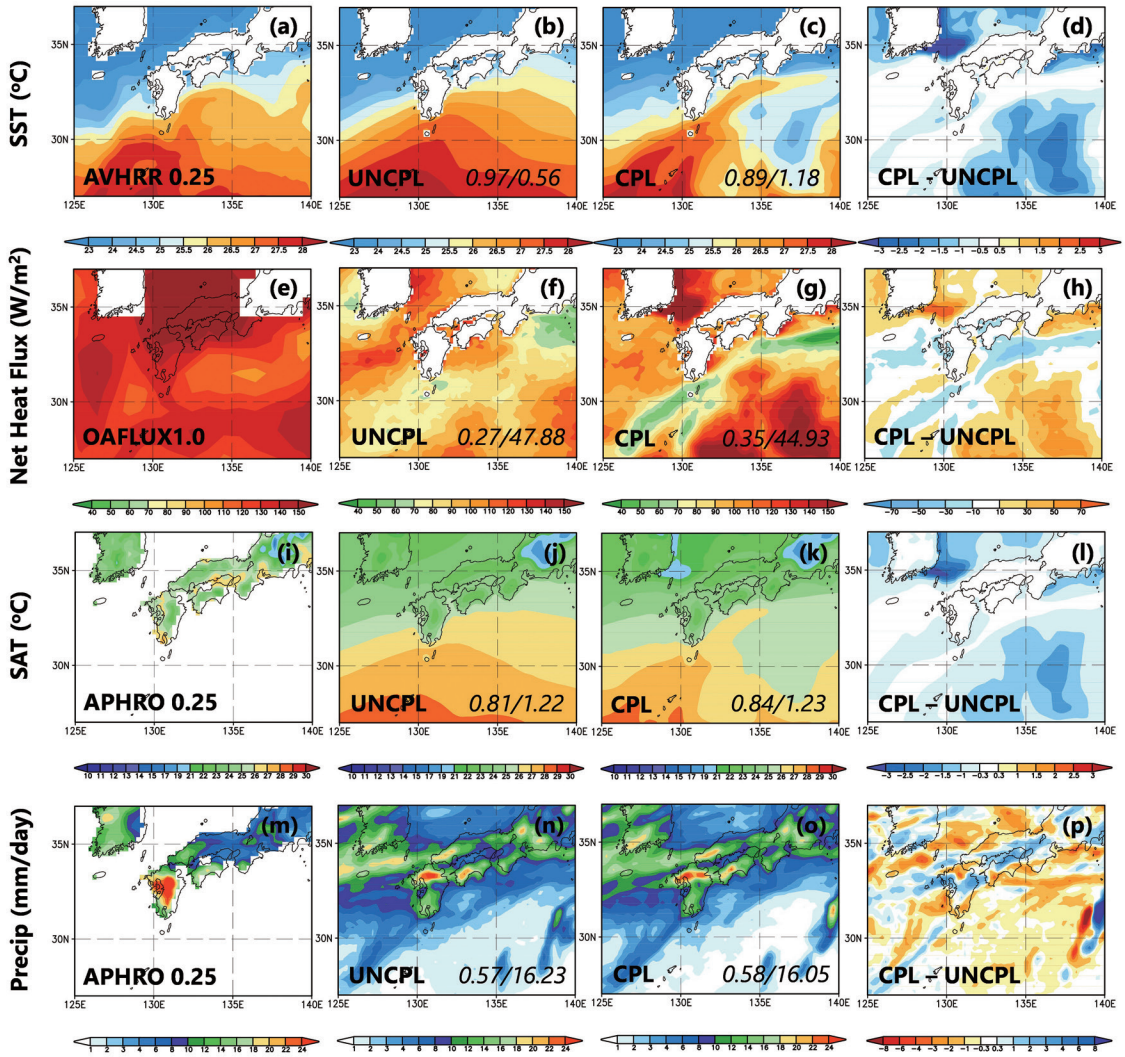

Fig. 5. Similar to Fig. 2, but for monthly mean (July 1987). SAT comparison is also included (i–l).

several of the typhoon cases, although the sea level pressure and wind variables are similar to each experiment. However, further understanding and investigation of the feedback mechanisms between typhoon and oceanic processes based on its track and intensity are needed.

4. Summary and conclusions

This note presents results of the first application of the recently developed atmosphere–ocean-coupled regional model system RSM–ROMS to the East Asian domain and provides comparisons and validations of SST, surface net heat fluxes, air temperature, and precipitation at both climatological and event-based scales. In short, the A–O coupling seems to have no or positive impact on net heat flux, SAT, and precipitation and no or negative impact on SST. The last is largely due to the fact that observed SST was used in the case of no coupling with a regional ocean model. However, although the large-scale horizontal distribution of SST was degraded, some improvement was observed at finer resolution, such as over coastal regions, by physically reasonable mechanisms, i.e., Ekman uplifting. The existence of an inverse relationship between degradation in SST and improvement in net heat flux may indicate that there is room for further improvement in coupling processes and boundary layer processes for both the atmosphere and

ocean. Furthermore, to reduce the biases of SST in the coupled run, it is essential to improve the cloud-radiation processes in the atmosphere model because SST is mainly determined by the heat fluxes as well as precipitation. Additionally, the impact of ocean circulation analysis on air–sea coupling, such as for SST, heat transfer, and mixed layer depth, is still under debate, despite the positive effect on atmospheric circulation. Further understanding of the feedback mechanisms between the atmosphere and ocean is needed.

Acknowledgments

This article includes studies conducted under the SOUSEI program of the Ministry of Education, Culture, Sports, Science and Technology in Japan (MEXT), the CREST program of the Japan Science and Technology Agency (JST), and the Japan Society for the Promotion of Science (JSPS) grants 23226012 and 26289160. The global ocean heat flux products were provided by the WHOI OAFlux project (http://oaflux.whoi.du) funded by the NOAA Climate Observations and Monitoring (COM) program.

References

Carton, J. A., G. Chepurin, X. Cao, and B. Giese, 2000: A simple ocean data assimilation analysis of the global upper ocean 1950–1995. Part I: Methodology. *J. Phys. Oceanogr.*, **30**, 294–309.

Chou, M.-D., 1992: A solar radiation model for use in climate studies. *J. Atmos. Sci.*, **49**, 762–772.

Chou, M.-D., K.-T. Lee, S.-C. Tsay, and Q. Fu, 1999: Parameterization for cloud longwave scattering for use in atmospheric models. *J. Climate*, **12**, 159–169.

DeHaan, L. L., and M. Kanamitsu, 2008: Increase in near surface temperature simulation skill due to predictive soil moisture in a numerical seasonal simulation under observed SST forcing. *J. Hydrometeor.*, **9**, 48–60.

Döscher, R., U. Willén, C. Jones, A. Rutgersson, H. E. M. Meier, U. Hansson, and L. P. Graham, 2002: The development of the coupled ocean-atmosphere model RCAO. *Boreal Environ. Res.*, **7**, 183–192.

Ek, M. B., K. E. Mitchell, Y. Lin, E. Rogers, P. Grunmann, V. Koren, G. Gayno, and J. D. Tarpley, 2003: Implementation of Noah land surface model advances in the National Centers for Environmental Prediction operational mesoscale Eta model. *J. Geophys. Res.*, **108**, 8851, doi:10.1029/2002JD003296.

Giorgi, F., and G. T. Bates, 1989: The climatological skill of a regional model over complex terrain. *Mon. Wea. Rev.*, **117**, 2325–2347.

Gustafsson, N., L. Nyberg, and A. Omstedt, 1998: Coupling of a high-resolution atmospheric model and an ocean model for the Baltic Sea. *Mon. Wea. Rev.*, **126**, 2822–2846.

Ham, S., S.-Y. Hong, and S. Park, 2014: A study on air–sea interaction on the simulated seasonal climate in an ocean–atmosphere coupled model. *Climate Dyn.*, **42**, 1175–1187.

Ham, S., J.-W. Lee, and K. Yoshimura, 2015: Assessing future climate changes in the East Asian summer and winter monsoon using a regional spectral model. *J. Meteor. Soc. Japan*, **94A**, 69–87.

Hodur, R. M., 1997: The Naval Research Laboratory's coupled ocean/atmosphere mesoscale prediction system (COAMPS). *Mon. Wea. Rev.*, **125**, 1414–1430.

Hong, S.-Y., and H.-L. Pan, 1996: Nonlocal boundary layer vertical diffusion in a medium-range forecast model. *Mon. Wea. Rev.*, **124**, 2322–2339.

Hong, S.-Y., and H.-L. Pan, 1998: Convective trigger function for a mass-flux cumulus parameterization scheme. *Mon. Wea. Rev.*, **126**, 2599–2620.

Hong, S.-Y., and E.-C. Chang, 2012: Spectral nudging sensitivity experiments in a regional climate model. *Asia-Pacific J. Atmos. Sci.*, **48**, 345–355.

Hong, S.-Y., and M. Kanamitsu, 2014: Dynamical downscaling: Fundamental issues from an NWP point of view and recommendations. *Asia-Pacific J. Atmos. Sci.*, **50**, 83–104.

Hong, S.-Y., H.-M. H. Juang, and Q. Zhao, 1998: Implementation of prognostic cloud scheme for a regional spectral model. *Mon. Wea. Rev.*, **126**, 2621–2639.

Huffman, G. J., R. F. Adler, M. M. Morrissey, D. T. Bolvin, S. Curtis, R. Joyce, B. McGavock, and J. Susskind, 2001: Global precipitation at one-degree daily resolution from multisatellite observations. *J. Hydrometeor.*, **2**, 36–50.

Kanamitsu, M., W. Ebisuzaki, J. Woollen, S.-K. Yang, J. J. Hnilo, M. Fiorino, and G. L. Potter, 2002: NCEP–DOE AMIP-II reanalysis (R-2). *Bull. Amer. Meteor. Soc.*, **83**, 1631–1643.

Kanamitsu, M., H. Kanamaru, Y. Cui, and H. Juang, 2005: *Parallel implementation of the regional spectral atmospheric model*. Scripps Institution of Oceanography, University of California, and National Oceanic and Atmospheric Administration for the California Energy Commission, PIER Energy-Related Environmental Research. CEC-500-2005-014.

Large, W. G., J. C. McWilliams, and S. C. Doney, 1994: Oceanic vertical mixing: A review and a model with a nonlocal boundary layer parameterization. *Rev. Geophys.*, **32**, 363–403.

Leung, L. R., and S. J. Ghan, 1995: A subgrid parameterization of orographic precipitation. *Theor. Appl. Climatol.*, **52**, 95–118.

Li, H., and V. Misra, 2014: Thirty-two-year ocean-atmosphere coupled downscaling of global reanalysis over the Intra-American Seas. *Climate Dyn.,* **43**, 2471–2489.

Li, H., M. Kanamitsu, and S.-Y. Hong, 2012: California reanalysis downscaling at 10 km using an ocean-atmosphere coupled regional model system. *J. Geophys. Res.*, **117**, D12118, doi:10.1029/2011JD017372

Li, H., M. Kanamitsu, S.-Y. Hong, K. Yoshimura, D. R. Cayan, and V. Misra, 2014a: A high-resolution ocean-atmosphere coupled downscaling of the present climate over California. *Climate Dyn.*, **42**, 701–714.

Li, H., M. Kanamitsu, S.-Y. Hong, K. Yoshimura, D. R. Cayan, V. Misra, and L. Sun, 2014b: Projected climate change scenario over California by a regional ocean-atmosphere coupled model system. *Climatic Change,* **122**, 609–619.

Marchesiello, P., J. C. McWilliams, and A. Shchepetkin, 2003: Equilibrium structure and dynamics of the California Current System. *J. Phys. Oceanogr.*, **33**, 753–783.

Mellor, G. L., and T. Yamada, 1982: Development of a turbulence closure model for geophysical fluid problems. *Rev. Geophys. Space Phys.*, **20**, 851–875.

Minamide, M., and K. Yoshimura, 2014: Orographic effect on the precipitation with Typhoon Washi in the Mindanao Island of the Philippines. *SOLA*, **10**, 67–71.

Pierce, D. W., D. R. Cayan, T. Das, E. P. Maurer, N. L. Miller, Y. Bao, M. Kanamitsu, K. Yoshimura, M. A. Snyder, L. C. Sloan, G. Franco, and M. Tyree, 2013: The key role of heavy precipitation events in climate model disagreements of future annual precipitation changes in California. *J. Climate*, **26**, 5879–5896.

Powers, J. G., and M. T. Stoelinga, 2000: A coupled air–sea mesoscale Model: Experiments in atmospheric sensitivity to marine roughness. *Mon. Wea. Rev.*, **128**, 208–228.

Reynolds, R. W., and T. M. Smith, 1994: Improved global sea surface temperature analyses using optimum interpolation. *J. Climate*, **7**, 929–948.

Reynolds, R. W., T. M. Smith, C. Liu, D. B. Chelton, K. S. Casey, and M. G. Schlax, 2007: Daily high-resolution blended analyses for sea surface temperature. *J. Climate*, **20**, 5473–5496.

Saha, S., S. Moorthi, H.-L. Pan, X. Wu, J. Wang, S. Nadiga, P. Tripp, R. Kistler, J. Woollen, D. Behringer, H. Liu, D. Stokes, R. Grumbine, G. Gayno, J. Wang, Y.-T. Hou, H.-Y. Chuang, H.-M. H. Juang, J. Sela, M. Iredell, R. Treadon, D. Kleist, P. van Delst, D. Keyser, J. Derber, M. Ek, J. Meng, H. Wei, R. Yang, S. Lord, H. V. D. Dool, A. Kumar, W. Wang, C. Long, M. Chelliah, Y. Xue, B. Huang, J.-K. Schemm, W. Ebisuzaki, R. Lin, P. Xie, M. Chen, S. Zhou, W. Higgins, C.-W. Zou, Q. Liu, Y. Chen, Y. Han, L. Cucurull, R. W. Reynolds, G. Rutledge, and M. Goldberg, 2010: The NCEP Climate Forecast System Reanalysis. *Bull. Amer. Meteor. Soc.*, **91**, 1015–1057.

Samala, B. K., N. C., S. Banerjee, A. Kaginalkar, and M. Dalvi, 2013: Study of the Indian summer monsoon using WRF–ROMS regional coupled model simulations. *Atmos. Sci. Lett.*, **14**, 20–27.

Sasaki, H., K. Kurihara, I. Takayabu, K. Murazaki, Y. Sato, and H. Tsujino, 2006: Preliminary results from the coupled atmosphere-ocean regional climate model at the Meteorological Research Institute. *J. Meteor. Soc. Japan*, **84**, 389–403.

Schrum, C., U. Hübner, D. Jacob, and R. Podzun, 2003: A coupled atmosphere/ice/ocean model for the North Sea and Baltic Sea. *Climate Dyn.*, **21**, 131–151.

Seo, H., A. J. Miller, and J. O. Roads, 2007: The Scripps Coupled Ocean-Atmosphere Regional (SCOAR) model, with applications in the eastern Pacific sector. *J. Climate*, **20**, 381–402.

Shchepetkin, A. F., and J. C. McWilliams, 2005: The regional oceanic modeling system (ROMS): A split-explicit, free-surface, topography-following-coordinate oceanic model. *Ocean Modelling*, **9**, 347–404.

Wada, A., and N. Usui, 2007: Importance of tropical cyclone heat potential for tropical cyclone intensity and intensification in the Western North Pacific. *J. Oceanogr.*, **63**, 427–447.

Xie, S.-P., T. Miyama, Y. Wang, H. Xu, S. P. de Szoeke, R. J. O. Small, K. J. Richards, T. Mochizuki, and T. Awaji, 2007: A regional ocean–atmosphere model for eastern Pacific climate: Toward reducing tropical biases. *J. Climate*, **20**, 1504–1522.

Yatagai, A., K. Kamiguchi, O. Arakawa, A. Hamada, N. Yasutomi, and A. Kitoh, 2012: APHRODITE: Constructing a long-term daily gridded precipitation dataset for Asia based on a dense network of rain gauges. *Bull. Amer. Meteor. Soc.*, **93**, 1401–1415.

Yoon, J.-H., L. R. Leung, and J. Correia., Jr., 2012: Comparison of dynamically and statistically downscaled seasonal climate forecasts for the cold season over the United States. *J. Geophys. Res.*, **117**, D21109, doi:10.1029/2012JD017650.

Zou, L., and T. Zhou, 2011: Sensitivity of a regional ocean-atmosphere coupled model to convection parameterization over western North Pacific. *J. Geophys. Res.*, **116**, D18106, doi:10.1029/2011JD015844.

Zou, L., and T. Zhou, 2012: Development and evaluation of a regional ocean-atmosphere coupled model with focus on the western North Pacific summer monsoon simulation: Impacts of different atmospheric components. *Sci. China Earth Sci.*, **55**, 802–815.